Acta Technica *62* No. 2B/2017, 733–742

Mapping data acquisition and processing of hybrid small unmanned aerial vehicle (UAVs)

Chen Chen[1]

Abstract. Unmanned aerial vehicle (UAV) is becoming more and more popular and recognized, and it can be used in many situations, such as search, rescue, surveillance and mobile sensor networks. In this paper, the automatic analysis of moving objects was introduced to generate real-time road points for the design and implementation of the four-rotating machines that the continuous reconnaissance was interested in. The system was equipped with an autopilot that controlled flight and on-board image processors. The processor analyzed the image to create a real-time estimate of the target's direction and speed. An algorithm for creating flight plans from captured imaging data was described. In addition, an algorithm for generating optimal trajectories through position and yaw angle sequences was developed.

Key words. Hybrid power, small unmanned aerial vehicle (UAV), mapping, data acquisition, processing methods.

1. Introduction

UAV is becoming more and more popular and recognized, and it can be applied to many occasions, such as search, rescue, surveillance and mobile sensor networks [1]. UAVs currently used for military surveillance applications include MQ-9, Reaper, RQ-7, Shadow, and RQ-11 Raven [2]. These systems include aircraft with sensor packages and data links for transmitting sensor data to related ground stations. The aim is to provide combat personnel with almost real-time situational awareness of battlefield [3]. As of 2010, the United States Army has been more than 4000 unmanned aircraft systems, and more programs for developing military drones.

Current UAV system technology has been able to autonomously operate, including automatic takeoff and landing, or following flight plans. The ground control station (GCS) is used to receive data collected from the system and control the UAS [4]. The project aims to increase autonomy in the control of UAV Systems and reduce the workload of combat personnel [5]. The ability to automatically process

[1]Hebei University of Water Resources and Electric Engineering, Cangzhou, Hebei, China, 061001

UAS sensor data is a key function in urban environments or indoor operations. With the development of embedded system technology, sensor data can be processed on chip to determine the required motion for UAS [6]. This increases the degree of autonomy that the system can operate and allows the user to receive data without the need to control the UAS.

2. State of the art

Recently, with the advent of modern microcontrollers and advances in sensor technology, an upsurge in the design of four rotors has been brought about. Today, there are more and more suppliers and platforms in the machine market. The use and application of these platforms are being studied and extended [7]. Multi-users usually provide high flexibility at the expense of search scope. Multiple helicopters must have the lift generated by propellers, and they are dominated by the wings (such as fixed wing aircraft) [8]. A company in San Francisco aims to transport food through the use of multiple devices. These innovative platforms are also frequently used in some unexpected places [9].

Obtaining flight performance and aerodynamic data for small UAVs is a complex task because of UAV size constraints, weight constraints, and power limitations [10]. The integration of sensors and flight controllers is another issue. Most commercial drones have their own data acquisition systems. These systems usually include the inertial measurement unit (IMU) with six or ten degrees of freedom, GPS modules with dedicated uplink and downlink, pilot probe or ground control station (GCS) [11]. Small UAVs for research purposes are expensive, which is a complex task. There are many devices on the international market to monitor the flight performance of non-commercial UAVs. Low-cost flight data monitoring system has great research significance because most of the equipment is expensive.

2.1. Methodology

2.2. System architecture for UAVs

The first is the weight based airframe design that uses MathCAD to optimize the target weight of the four rotators. Manufacturers estimate that each engine produces about 1000 g of thrust combined with 8×4.3 propellers. Four motors provide a total of 4000 g of thrust to lift the fuselage. The manufacturer cannot obtain the torque curve, so four rotators are selected at a 45 % duty ratio. Autodesk Inventor is used to estimate the total weight of the components, calculate 1800 grams of thrust and give about 4 pounds of target weigh.

The picture of the investigated microdrone is in Fig. 1

The system contains an Arduino compatible GPS/GPRS/GSM module that is used to locate the drone's GPS capabilities. The compact IMU sensor SEN-00126 with ten degrees of freedom (10-DOF) is selected. The sensor is a combination of MPU9255 sensors and BMP180 sensors. The MPU9255 sensor can measure 9 inertial parameters: 3 axial angular accelerations, 3 axial gyroscopic motions (scroll,

Fig. 1. Microdrone md4-200 with a Ricoh GR3 compact camera

pitch and yaw), and 3 axial magnetic/Compass headings. The BMP180 is an atmospheric pressure sensor that measures airspeed in terms of pressure. Using IMU sensors instead of accelerometers alone, gyroscopes, magnetometers, and barometers can reduce circuit complexity, and consume less space and cost effectiveness. The Arduino SD card module is used as a data logger for transmitting data from various sensors and stored in SD cards. One of the most important goals of this research is to reduce costs rather than using expensive commercial data acquisition devices. Therefore, locally available and cost effective hardware is selected. Obtaining flight performance and aerodynamic data for small UAVs is a complex task because of UAV size constraints, weight constraints, and power limitations. The integration of sensors and flight controllers is another issue. Most commercial drones have their own data acquisition systems. These systems usually include the inertial measurement unit (IMU) with six or ten degrees of freedom, the GPS module with dedicated uplink and downlink, pilot probe or ground control station (GCS).

The drive uses the ArduCopter suite. The software set used by the autopilot is an open source project called ArduCopter (ArduCopter 2012). ArduCopter aims to create an easy to install and fly platform for multi-rotor UAVs. The project provides software for controlling helicopters in flight. The interface of RC receiver allows manual control and coverage. For debugging purposes, the Bluetooth link is used as a wireless serial data link to the ground station. ArduCopter is a popular project that receives regular updates from its developers. The version 2.0.48 is the latest version of APM. As of May 2012, the 2.5.5 version was widely used.

The open source projects are used for project design, and it provides a GUI interface to configure APM, monitor flight status, enter waypoints, analyze log files and change flight patterns. The software is used for functional testing APM, and loading firmware changes, which usually runs on the Windows desktop. Although Mono is running on other operating systems (Ardupilot itself uses program mono 2011 on the Ubuntu Linux), the scheduler cannot run on the development board under Linux.

The power distribution system must provide sufficient current for all critical flight components, so as to achieve a successful flight. The main power comes from two

12 V lithium polymer batteries. The capacity of each battery is 5000mAh, and the rated power is 200 A for continuous discharge. The main load on the system is four motors. The maximum current consumption of each motor is 28 A when it is stopped. The load generated by the four motors is 112 A, which can be easily handled by a single battery. The power from the battery is fed to the four electronic speed controllers (ESC) via the power switch. Each ESC can continuously supply up to 30 A of an electric motor with a voltage of 12 V. Each ESC also offers 2 A in 5 V, which powers the autopilot and image processor. The four ESCs together create a 5 V track capable of 8 A. The autopilot and image processor are small loads that consume 3 % of the total power. The autopilot receives the 5 V power from the ESC. The image processor is connected to the 5 V rail on the autopilot. Although the ESCs filter most of the high frequency noise of the motor, it adds extra protection to the image processor. The LC filter between the autopilot and the image processor filters out any additional noise and stabilize the current. The overall power distribution block diagram is shown in Fig. 2.

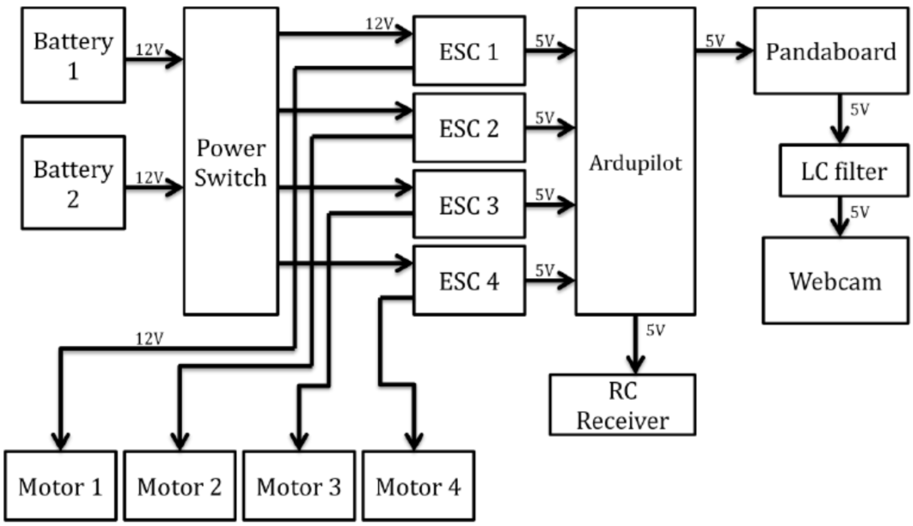

Fig. 2. Power distribution block diagram

2.3. Data acquisition system

In today's software projects, code modularity and reusability are always the most important. Because of the rapid development of hardware, evaluating a piece of code is not just about running speed, but modularity, reusability, and scalability. In order to meet these requirements, there are many options available in the data acquisition system. In this case, the actual observer is the specific sensor that is connected to the device. All sensors, regardless of their function, must implement an abstract interface that has the function of configuring and controlling sensors. The coordinators store the list of registered observers (devices). When it wants to control them, it will walk through the list and call one of the generic functions. The task of the coordinator is not to understand every particular detail of each additional device, but to implement and use well-defined interfaces that are used and known by the coordinator.

Imaging sensor is an important component of the system that provides imaging feedback to the image processor. After considering various imaging sensors, only video sensors are purchased due to cost. Cameras provide high quality video. However, due to 167 grams of high weight and unable to convert the output video stream to the Linux operating system in real time, the camera is replaced. Logitech C310 network camera is selected because it is low in weight and compatible with Linux (C310 technical specification 2012).

Next is the design of the UAV message marshalling library. The library is used to provide a two-way interface between the image processor and the autopilot. The protocol has the characteristics of high transmission speed and good security performance, so it is usually used in ground control station (GCS) to MAV architecture. Python scripts are used to implement protocols, and the language used is 8 bytes with a maximum payload of 255 bytes. The USB serial interface provides 115200 BPS of bandwidth per second, or about 56 MAVLink packets. In this application, the development board can send MAVLink messages to the APM of the four - way transponder. With the functions of the cover RC channel, more independent procedures are developed, and "arms" and "removal" functions are written. Various functions along with takeoff to a certain height are landed to achieve autonomy. Although a framework has been set up, further development is needed to create a fully autonomous product. The image processing software uses the supplied MAVLink code for processing and output.

Processing data captured from a camera to detect the target and its attributes. The image analysis identifies the position of the target relative to the four rotators and determines the set point required for the PID motion controller. OpenCV is a real-time computer vision library (OpenCV 2012). It contains an optimization algorithm for general image processing. All of the codes are written by C++ with OpenCV 2.3 version.

The camera is attached to the moving object for detecting and analyzing the operation of the object software under the Linux operating system, and the multiple iterations of the image detection software set are carried out. After the video stream is turned on, the image is resized to 320 pixels×240 pixels. Images are shielded by upper and lower bounds to isolate objects. The objects are successfully isolated in the image. The object is placed 5 meters away from the camera. The first method of motion analysis is by sensing the circular contour and recording the position in the loop buffer. The buffer is then used to calculate the movement of the target, and a block diagram of the data output is given below.

3. Result of analysis and discussion

The primary purpose of the first field test is to view and measure the range of the radio module. The test settings are made up of two design versions of PCB. One uses

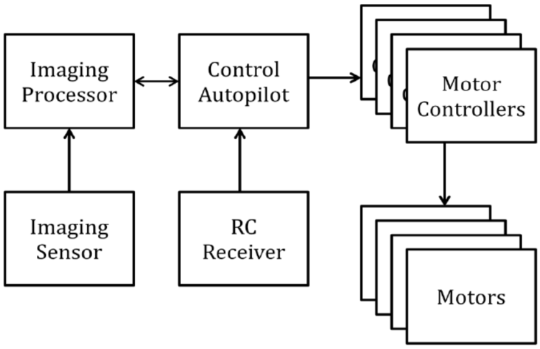

Fig. 3. Data flow diagram

the linear converter as the power source, and the other uses a buck converter. Test scenario: a node of communication is placed in the fix, and the predefined location is not move throughout the experiment. It is programmed to send data packets over a radio interface (Radiocrafts, RC-1280). The second sensor node has been installed with the GPS module. It is programmed to receive any incoming data from the wireless module and write the received data along with the timestamp and the GPS coordinates on the SD card. Basically, this test checks the functions of the SD card, the radio module, the GPS module, the voltage regulator, and several GPIO pins used to control certain states of the LED. The model after the overall installation is shown in Fig. 4.

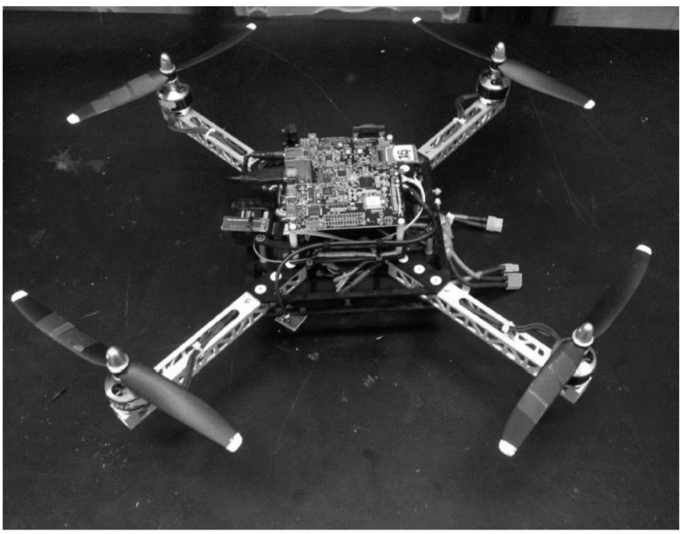

Fig. 4. Quadrotor airframe and electronics

After the sensor nodes are incorporated into the transmitted data, the second mobile sensor has moved from a distance of about 1 km from the fixed sensor. The test result is ideal: the maximum distance between the two modules is 660 m, which corresponds to the potential area of a circle with a diameter of 1.3 km. Although the test conditions are not ideal, the result makes it possible to successfully implement the effective communication between the UAV and the sensor nodes at that distance.

The next test is to check the feasibility of the entire communication process. The main difference from previous tests is that a test module is added to these tests. The UAV used is the X8 flying wing, and its active components include a development board and several mechanical/electrical modules. The program and setup use the DUNE software framework introduced in the previous chapter. The development board can run under the Linux system. And a DUNE task has been written to read the incoming data from the serial port and package it into the IMC message. Thereafter, the received message is transmitted to the DUNE via the 5 GHz link.

The sensor nodes are set up on the ground in advance, and each parameter is adjusted. The UAV is controlled to fly over it to collect its data and forward data to the base station. The next image shows a snapshot of the test process. In this test, the sensor nodes have been programmed to sample data. The collected data is sent to UAV as a sample and recorded on the SD card, and no sleep mode is adopted. The data sent by the sensor node is composed of temperature readings and their GPS coordinates. The UAV's development board starts running the DUNE task, reads data from the sensor nodes and records it. Some data is sent back to the sensor node. The received sensor data is forwarded to the base station by forwarding 5 Hz through the UDP connection. The base station is a computer that runs the DUNE software, and the comparison of the captured images is shown in Fig. 5.

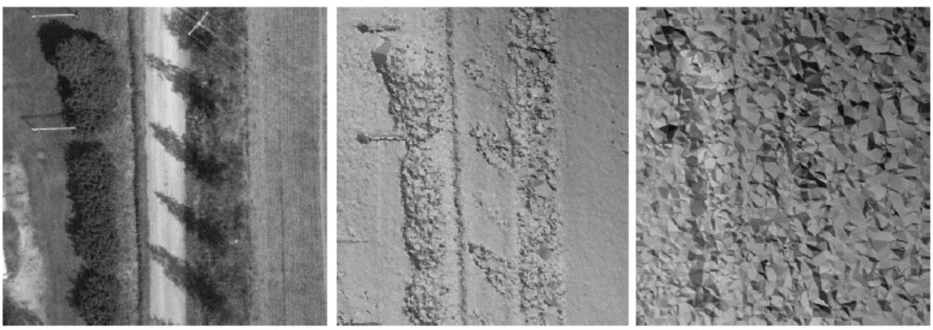

Fig. 5. Image acquisition contrast

The test takes 14 minutes of flight time. During the whole process, sensor nodes, UAVs and base stations have valid data links. Sensor nodes have been previously placed on the map representing the center of the red circle. The maximum distance between the UAV and the sensor node is 100 m on the horizontal axis, and the height is 100 m. The number of messages sent from the sensor node to the UAV (GPS position and temperature) is about 438. All of these messages are accompanied by check and field, and they are checked only once throughout the flight. It means that the packet lost from the sensor node to the UAV is the smallest. There are different cases in which messages are sent back from the UAV to the sensor nodes. Packets sent from UAV to sensor nodes should be commands and configuration files. In this test scenario, the received data (command) is not explained explicitly and is directly logged on the SD card. The results are also good. In Table 1, the received data is edited and compared to the actual data. Because the CRC field is not added to these packets, the damaged field is recorded. In the range of 3 m×3 m, the relative density of the acquired images is evaluated, and the results are as follows. It can be seen that the collection situation is different in different areas, and the relative density of different objects is different. From the results of the table, it can be seen that the collected density is relatively large, which can reach 0.87–0.90.

Table 1. Points per square meter and relative point densities evaluated in different objects in 3 m×3 m areas

	Points per square meter				Relative point density			
	Field	Grass	Forest	Asphalt	Field	Grass	Forest	Asphalt
UC NGATE	82.1	86.9	47.6	89.6	0.82	0.87	0.48	0.90
GF NGATE	278.2	361.8	136.0	233.0	0.70	0.90	0.34	0.58
Photosynth	2.9	2.4	2.1	2.4	-	-	-	-

4. Conclusion

So far, autonomic search and tracking models have been successfully simulated. In this paper, the automatic analysis of moving objects was introduced to generate real-time road points for the design and implementation of the four-rotating machines that the continuous reconnaissance is interested in. The system is equipped with an autopilot that controls flight in flight and on-board image processors. Simulations can reach maturity that accurately reflects the intent of the action language model. Both models and simulations provide a powerful basis for allowing the development of autonomous agents for a variety of applications. The current prototype is able to stabilize flight and provide sufficient battery life and agility for further development. The components of the problem are usually motors and propellers. Platforms do not have built-in redundancy, and problems that occur can lead to catastrophic failures. Motor faults are traced to connectors that fail at high vibration, thus resulting in intermittent signal integrity problems. These connector failures cause a sharp drop in the motor RPM and crash, and the basic design is carried out from the APM and development boards. Although some achievements are made in image processing software and data acquisition system, it needs further improvement, such as object recognition and so on.

References

[1] D. H. Ho, P. B. Sujit, T. A. Johansen, J. B. Sousa: *Optimization of wireless sensor network and UAV data acquisition.* Journal of Intelligent & Robotic Systems *78* (2015), No. 1, 159–179.

[2] S. Say, H. Inata, J. Liu, S. Shimamoto: *Priority-based data gathering framework*

in UAV-assisted wireless sensor networks. IEEE Sensors Journal *16* (2016), No. 14, 5785–5794.

[3] A. Mazayev, N. Correia, G. Schütz: *Data gathering in wireless sensor networks using unmanned aerial vehicles*. International Journal of Wireless Information Networks *23* (2016), No. 4, 297–309.

[4] I. Jawhar, N. Mohamed, J. Al-Jaroodi, S. Zhang: *A framework for using unmanned aerial vehicles for data collection in linear wireless sensor networks*. Journal of Intelligent & Robotic Systems *74* (2014), Nos. 1–2, 437–453.

[5] L. A. Villas, D. L. Guidoni, G. Maia, R. W. Pazzi, J. Ueyama, A. A. F. Loureiro: *An energy efficient joint localization and synchronization solution for wireless sensor networks using unmanned aerial vehicle*. Wireless Networks *21* (2015), No. 2, 485–498.

[6] C. Keleshis, S. Ioanno, M. Vrekoussis, Z. Levin, M. A. Lange: *Data Acquisition (DAQ) system dedicated for remote sensing applications on Unmanned Aerial Vehicles (UAV)*. International Conference on Remote Sensing and Geoinformation of the Environment, 12 August 2014, Paphos, Cyprus, Proceedings of SPIE *9229* (2014).

[7] G. Bareth, A. Bolten, M. L. Gnyp, S. Reusch, J. Jasper: *Comparison of uncalibrated RGBVI with spectrometer-based NDVI derived from UAV sensing systems on field scale*. ISPRS - International Archives of the Photogrammetry, Remote Sensing and Spatial Information Sciences *XLI-B8* (2016), 837–843.

[8] S. Say, M. E. Ernawan, S. Shimamoto,: *Cooperative path selection framework for effective data gathering in UAV-aided wireless sensor networkss*. IEICE Transactions on Communications *E99.B* (2016), No. 10, 2156–2167.

[9] F. Chiabrando, A. Spanò, G. Sammartano, L. T. Losè: *UAV oblique photogrammetry and lidar data acquisition for 3D documentation of the Hercules Fountain*. Virtual Archaeology Review *8* (2017), No. 16, 83–96.

[10] M. Smigaj, R. Gaulton, S. L. Barr, J. C. Suárez: *UAV-borne thermal imaging for forest health monitoring: Detection of disease-induced canopy temperature increase*. ISPRS - International Archives of the Photogrammetry, Remote Sensing and Spatial Information Sciences *XL-3/W3* (2015), 349–354.

[11] E. Honkavaara, H. Saari, J. Kaivosoja, I. Pölönen, T. Hakala, P. Litkey, L. Pesonen: *Processing and assessment of spectrometric, stereoscopic imagery collected using a lightweight UAV spectral camera for precision agriculture*. Remote Sensing *5* (2013), No. 10, 5006–5039.

Received October 10, 2017